International Journal of the Physical Sciences Vol. 5(5), pp. 507-517, May 2010
Available online at http://www.academicjournals.org/IJPS
ISSN 1992 - 1950 © 2010 Academic Journals

Full Length Research Paper

Modeling of penetration depth of air bubbles entrained by sharp crested weirs using ANFIS

Mehmet Unsal

Department of Civil Engineering, Kahramanmaras Sutcu Imam University, Kahramanmaras, Turkey.
E-mail: munsal@ksu.edu.tr.

Accepted 26 April, 2010

In rivers and streams aeration of water flows is very important to the quality and existence of aquatic life. Aeration is the process by which the area of contact between water and air is increased, either by natural methods or by mechanical devices. It is important in aeration process by which the area of contact and contact time between water and air. Increasing the contact time of air bubbles is proportional with penetration depth of air bubbles. In this study, the penetration depth of air bubbles entrained by sharp crested weirs is modeled by using the adaptive network based fuzzy inference system (ANFIS). The obtained model was tested with experimental data. There was a good agreement between model and experimental data. Test results showed that ANFIS can be used to estimate the penetration depth of air bubbles entrained by sharp crested weirs.

Key words: Sharp crested weir, aeration, penetration depth, ANFIS.

INTRODUCTION

Dissolved oxygen (DO) is essential to healthy river, streams and lakes. The presence of oxygen in water is a positive sign and the absence of oxygen is a sign of severe pollution. Many naturally occurring biological and chemical processes use oxygen, thereby decreasing the DO concentration in water. The physical process of oxygen transfer or oxygen absorption from the atmosphere acts to replenish the used oxygen. This process has been termed reaeration or aeration (Baylar and Emiroglu, 2004).

Hydraulic structures have an impact on the amount of dissolved oxygen in a river system, even though the water is in contact with the structure for only a short time. The same quantity of oxygen transfer that normally would occur over several kilometers in a river can occur at a single hydraulic structure. The primary reason for this accelerated oxygen transfer is that air is entrained into the flow, which produces a large number of bubbles. These air bubbles greatly increase the surface area available for mass transfer (Baylar and Bagatur, 2000).

Weir aeration occurs in rivers, fish hatcheries and water treatment plants. The flow over a weir can be classified as a free jet. The free jet plunging the air bubbles into a downstream water pool. These air bubbles reach to a certain depth in downstream pool. The distance between the certain depth and water surface called penetration depth (Figure1).

The residence time of entrained air bubbles in a water body directly affects the oxygen mass transfer. The residence time is related to the bubble flow path and hence the bubble penetration depth into the downstream water pool. As the contact time between bubbles and water body increases the aeration performance increase (Baylar and Bagatur, 2000).

Aeration performance and aeration efficiency of two-phase flow have been studied experimentally by a number of investigators. These studies are reviewed by Gulliver et al. (1990), Gulliver et al. (1993), Avery and Novak (1978), Baylar (2002), Baylar (2003), Baylar and Bagatur (2000), (2006), Baylar and Emiroglu (2002), Emiroglu and Baylar (2003), Chanson (1995), Wormleaton and Tsang (2000), Ito et al. (2000).

Intelligent methods are widely used in various areas of water-related research (ASCE, 2000; Kisi, 2004a - b; Abolpour et al., 2007). For modeling aeration efficiency of hydraulic structures different intelligent methods were used (Baylar et al., 2007: Hanbay et al., 2006a-b). In this

Abbreviation: ANFIS, Adaptive network based fuzzy inference system.

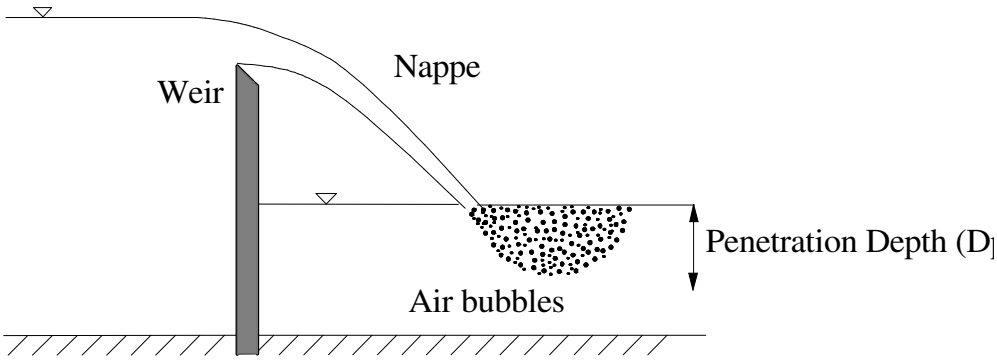

Figure 1. Penetration depth in sharp crested weir.

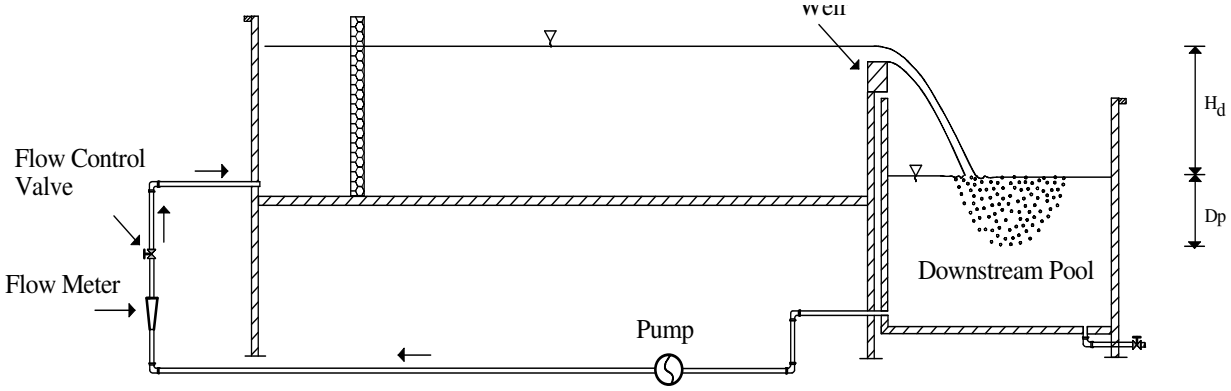

Figure 2. Experimental setup.

study, the penetration depth of air bubbles entrained by sharp crested weirs was modeled by using the adaptive network based fuzzy inference system (ANFIS).

EXPERIMENTAL SETUP

The data used in this study were taken from a study conducted by Emiroglu (2010). Schematic representation of the experimental setup is shown on Figure 2. In experimental setup flow meter, flow control valve and pump were used. Experiments were conducted in hydraulic laboratory at the Engineering Faculty of Firat University, Elazig, Turkey. The experimental channel used in this study was 3.40 m long, 0.60 m wide and 0.50 m deep with a maximum water flow rate of 5 L/s. The water in the experimental channel was circulated by a pump. The plan-view dimensions of the downstream pool were 1.20 × 1.20 m.

The weirs used in experiments were: the rectangular sharp-crested weirs with B_w = 10, 20 and 30 cm; the triangular sharp-crested weirs with four V-notches; the 30° triangular sharp-crested weir; the 60° triangular sharp-crested weir; the 90° triangular sharp-crested weir and the 120° triangular sharp-crested weir; the trapezoidal sharp-crested weir; and the semicircular sharp-crested weir as shown in Figure 3a - d.

Each sharp-crested weir configuration was tested under flow rates Q varying from 1.0 to 5.0 in 1 L/s steps. The drop height H_d, defined as the difference between the water levels upstream and downstream of the sharp-crested weir, was varied from 0.20 to 1.0 in 0.20 m steps.

F_j = jet Froude number = $\left[\frac{g\,Hd^{3}}{2q_j^{2}}\right]^{1/4}$;

Re_j = jet Reynolds number= $\frac{q_j}{\nu}$ ($\nu = \mu/\rho$) were calculated

Where, q_j = discharge through the per unit water surface width at the crest of the weir ($q_j = Q/B_w$; Q = total discharge through the weir); g = gravity acceleration; μ = viscosity of water. The penetration depth of air bubbles was measured in downstream pool for each type of sharp crested weir.

Adaptive network based fuzzy inference system (ANFIS)

The architecture and learning rule of adaptive network based fuzzy inference system (ANFIS) were described in detail in Jang (1993). ANFIS is a multilayer feed forward network where each node performs a particular function on

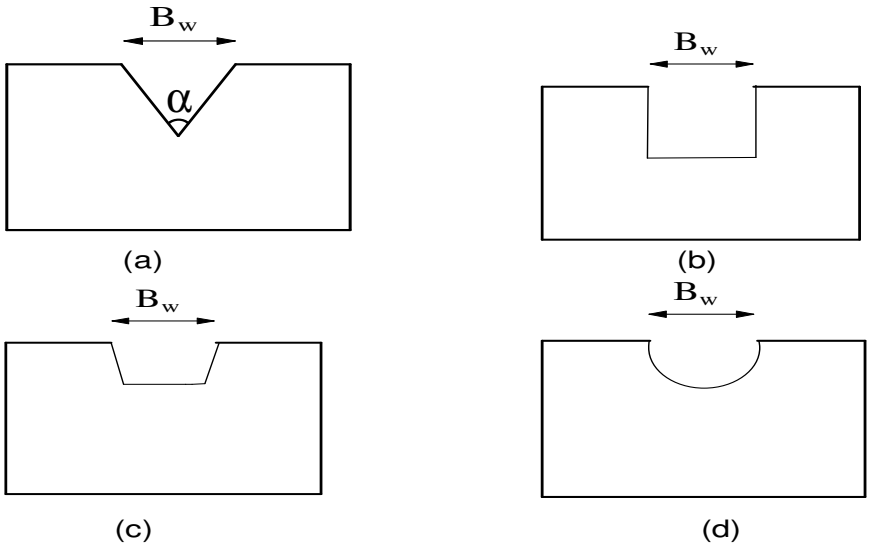

Figures 3a – d. Weir types (a- Triangular sharp-crested weir, b- Rectangular sharp-crested weir, c- Trapezoidal sharp-crested weir, d- Semi circular sharp-crested weir)

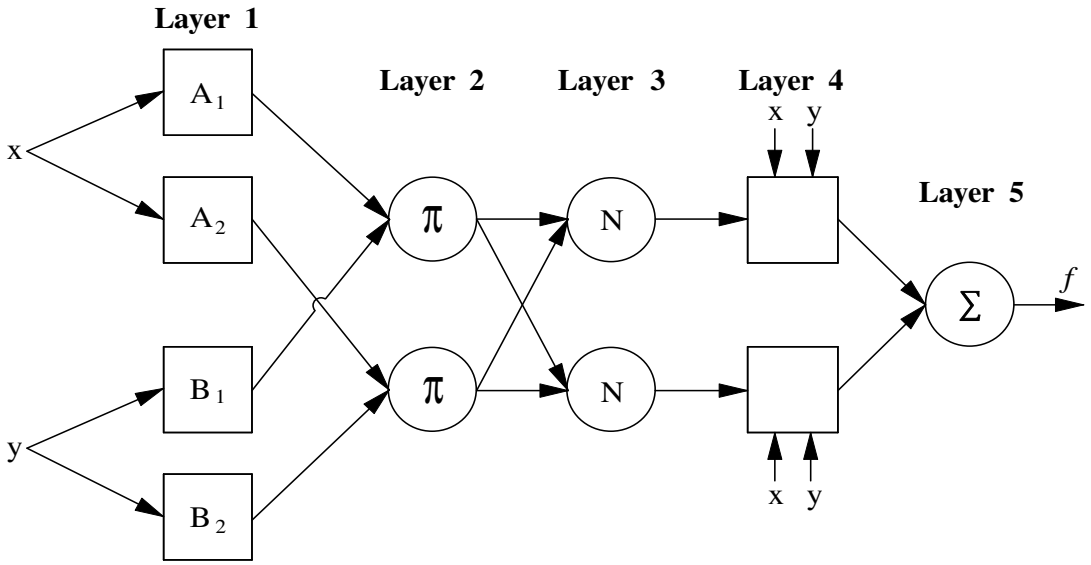

Figure 4. ANFIS model structure.

incoming signals. Both square and circle node symbols are used to represent different properties of adaptive learning. To perform desired input and output characteristics, adaptive learning parameters are updated based on gradient learning rules. To describe ANFIS architecture, we assume a fuzzy inference system under consideration has two inputs *x* and *y* and one output *z*. ANFIS model is one of the implementation of a first order Sugeno fuzzy inference system (Kulkarni, 2001). The rules are of the form Equation 1 in this system".

Rule *1*: If *x* is A_1 and *y* is B_1, then $f_1 = p_1x + q_1y + r_1$,

Rule 2: If *x* is A_2 and *y* is B_2, then

$$f_2 = p_2x + q_2y + r_2 . \quad (1)$$

Where *A* and *B* corresponding term set, *f* is output and, *p, q, r* are constant.

An ANFIS model is shown in Figure 4. It is a multi–input, one–output model however a multi–output model can be designed by connecting few single output models. The node functions in the same layer are similar and described as below:

Layer–1: Every node *i* in this layer is a square node with a node function. Nodes in layer 1 implement fuzzy membership functions, mapping input variables to corresponding fuzzy membership values. Outputs of this layer can be described by Equation 2

$$O_i^1 = \mu A_i(x) \quad (2)$$

where, *x* is input to node *i* and A_i is linguistic label associated with this node function. O_i^1 is the membership function of A_i, the fuzzy Membership Functions (MF) can take any form, such as triangular, Gaussian but usually $\mu A_i(x)$ is chosen bell–shaped with maximum equal to 1 and minimum equal 0.

Layer–2: Every node in this layer is a circle node labeled Π which multiplies the incoming signals and sends the product out. For instance,

$$w_i = \mu A_i(x) \times \mu B_i(y), \quad i=1, 2 \quad (3)$$

Each node output represents the firing strength of a rule.

Layer–3: Every node in this layer is a circle node labeled *N*. The i_{th} node calculates the ratio of the i_{th} rules firing strength to the sum of all rule's firing strengths.

$$\overline{w}_i = \frac{w_i}{w_1 + w_2} \quad i=1, 2 \quad (4)$$

For convenience, outputs of this layer will be called normalized firing strengths.

Layer–4: Every node *i* in this layer is a square node with a node function,

$$O_i^4 = \overline{w}_i f_i = \overline{w}_i (p_i x + q_i y + r_i) \quad (5)$$

where $\overline{w}_i$ is the output of layer 3 and $\{p_i, q_i, r_i\}$ is the parameter set. Parameters in this layer will be referred to as consequent parameters.

Layer–5: The single node in this layer is a circle node labeled ∑ that computes the overall output of ANFIS as the summation of all incoming signals.

$$O_i^5 = overalloutput = \sum_i \overline{w}_i f_i = \frac{\sum_i w_i f_i}{\sum_i w_i} \quad (6)$$

ANFIS applications

All ANFIS models were realized with MATLAB. Three Gauss2mf type membership functions were used for each input to predict D_p with 500 training epochs. 3–fold cross validation method is applied to evaluate the test performance of ANFIS models. The test performances were tabulated. In this study the best models performances are shown in Figures for each sharp crested weir type. In each stage, R^2 statistics were calculated.

Modeling for triangular weir type

In modeling stage, F_j, jet Froude number, Re_j, jet Reynolds number, H_d, drop height, α, angle in triangular sharp crested weir were used as models input parameters and D_p which indicates penetration depth was used as model output as shown in Table 1. The R^2 value was 0.97. There was a good agreement between experimental data and samples as seen in Figure 5.

Modeling for rectangular weir type

F_j, jet Froude number, Re_j, jet Reynolds number, H_d, drop height, B_w, water surface width over the crest of the weir were used as models input parameters and D_p which indicates penetration depth was used as model output as shown in Table 2. The R^2 value was 0.98. There was a good agreement between experimental data and samples as seen in Figure 6.

Modeling for trapezoidal weir type

F_j, jet Froude number, Re_j, jet Reynolds number, H_d, drop height, B_w, water surface width over the crest of the weir were used as models input parameters and D_p which indicates penetration depth was used as model output as shown in Table 3. The R^2 value was 0.94. There was a good agreement between experimental data and samples as seen in Figure 7.

Modeling for semi circular weir type

F_j, jet Froude number, Re_j, jet Reynolds number, H_d, drop height, B_w, water surface width over the crest of the weir were used as models input parameters and D_p which indicates penetration depth was used as model output as shown in Table 4. The R^2 value was 0.97. There was a good agreement between experimental data and samples as seen in Figure 8.

Table 1. Experimental data of sharp crested triangular weirs.

Hd. (cm)	Rej	Fj	Angle degree	Dp. (cm)	Hd. (cm)	Rej	Fj	Angle degree	Dp. (cm)
20	25138.24	2.779	30	40.5	20	10212.42	4.361	90	60.0
40	25138.24	4.675	30	43.0	40	10212.42	7.334	90	57.0
60	25138.24	6.336	30	24.5	60	10212.42	9.941	90	40.0
80	25138.24	7.862	30	23.5	80	10212.42	12.334	90	37.0
100	25138.24	9.294	30	20.5	100	10212.42	14.581	90	36.0
20	33806.67	2.397	30	43.0	20	18674.14	3.225	90	68.0
40	33806.67	4.031	30	45.0	40	18674.14	5.424	90	65.0
60	33806.67	5.464	30	33.5	60	18674.14	7.351	90	54.0
80	33806.67	6.779	30	24.5	80	18674.14	9.121	90	40.0
100	33806.67	8.014	30	23.5	100	18674.14	10.783	90	38.0
20	40849.71	2.180	30	36.5	20	24925.22	2.791	90	79.0
40	40849.71	3.667	30	52.0	40	24925.22	4.694	90	72.0
60	40849.71	4.970	30	30.5	60	24925.22	6.363	90	58.0
80	40849.71	6.167	30	29.5	80	24925.22	7.895	90	50.0
100	40849.71	7.291	30	25.5	100	24925.22	9.333	90	45.0
20	45599.61	2.064	30	52.0	20	29485.48	2.556	90	84.0
40	45599.61	3.471	30	54.5	40	29485.48	4.316	90	82.0
60	45599.61	4.704	30	41.0	60	29485.48	5.850	90	64.0
80	45599.61	5.834	30	29.5	80	29485.48	7.259	90	52.0
100	45599.61	6.900	30	30.5	100	29485.48	8.581	90	49.0
20	53282.18	1.909	30	53.0	20	33121.36	2.421	90	86.5
40	53282.18	3.211	30	35.5	40	33121.36	4.072	90	82.0
60	53282.18	4.352	30	40.0	60	33121.36	5.520	90	65.0
80	53282.18	5.400	30	33.0	80	33121.36	6.849	90	56.0
100	53282.18	6.384	30	30.5	100	33121.36	8.097	90	51.0
20	17507	3.331	60	42.5	20	6535.95	5.451	120	60.0
40	17507	5.602	60	30.0	40	6535.95	9.168	120	54.5
60	17507	7.592	60	26.0	60	6535.95	12.426	120	51.5
80	17507	9.421	60	27.0	80	6535.95	15.418	120	40.5
100	17507	11.137	60	24.0	100	6535.95	18.227	120	38.5
20	27233.12	2.670	60	55.5	20	10893.25	4.222	120	69.0
40	27233.12	4.491	60	45.0	40	10893.25	7.101	120	65.5
60	27233.12	6.087	60	34.0	60	10893.25	9.625	120	60.5
80	27233.12	7.553	60	33.0	80	10893.25	11.943	120	46.0
100	27233.12	8.929	60	30.0	100	10893.25	14.118	120	40.0
20	32679.74	2.438	60	56.5	20	14005.6	3.724	120	74.5
40	32679.74	4.099	60	46.5	40	14005.6	6.263	120	70.5
60	32679.74	5.557	60	32.0	60	14005.6	8.488	120	62.5
80	32679.74	6.895	60	32.5	80	14005.6	10.532	120	53.5
100	32679.74	8.151	60	27.5	100	14005.6	12.450	120	46.0
20	37707.39	2.269	60	63.0	20	16339.87	3.448	120	102.0
40	37707.39	3.817	60	48.5	40	16339.87	5.798	120	74.0
60	37707.39	5.173	60	35.5	60	16339.87	7.859	120	64.5
80	37707.39	6.419	60	34.0	80	16339.87	9.751	120	54.5
100	37707.39	7.588	60	30.5	100	16339.87	11.528	120	46.5
20	40180.01	2.199	60	65.0	20	18853.7	3.209	120	113.0
40	40180.01	3.697	60	53.0	40	18853.7	5.398	120	100.0
60	40180.01	5.012	60	36.5	60	18853.7	7.316	120	70.5
80	40180.01	6.218	60	36.0	80	18853.7	9.078	120	61.5
100	40180.01	7.351	60	33.0	100	18853.7	10.732	120	48.5

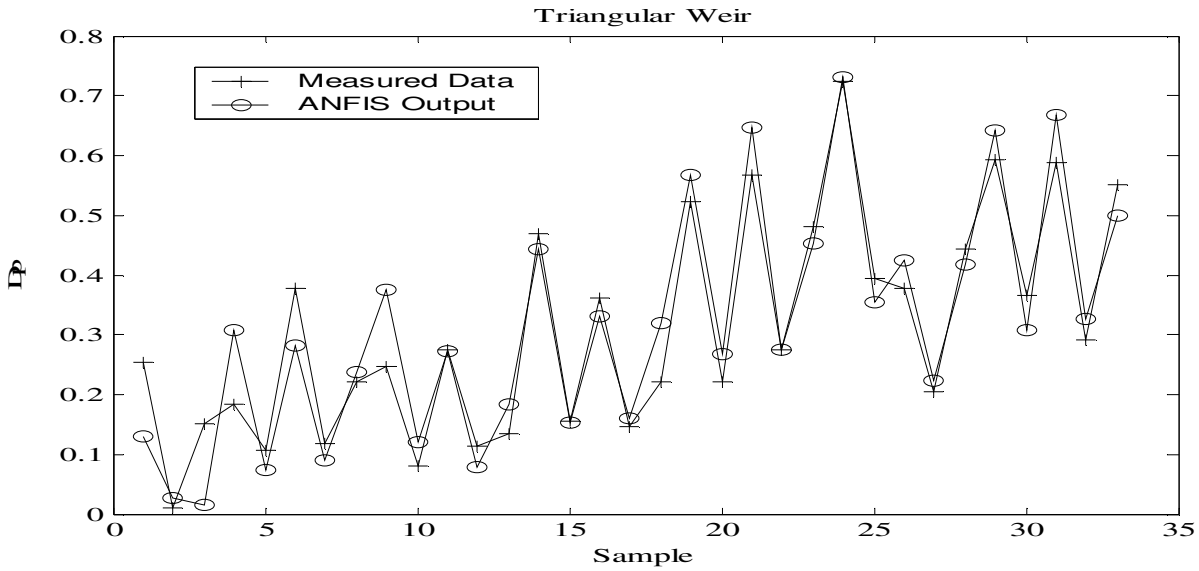

Figure 5. The predicted and measured D_p values in triangular weir.

Table 2. Experimental data of sharp crested rectangular weirs.

Hd. (cm)	Re	Fj	Bw. (cm)	Dp. (cm)
20	9803.92	4.451	10	95.0
40	9803.92	7.485	10	90.5
60	9803.92	10.145	10	82.0
80	9803.92	12.588	10	76.2
100	9803.92	14.882	10	58.9
20	19607.84	3.147	10	100.6
40	19607.84	5.293	10	100.0
60	19607.84	7.174	10	88.1
80	19607.84	8.901	10	71.0
100	19607.84	10.523	10	58.8
20	29411.76	2.570	10	100.5
40	29411.76	4.321	10	93.6
60	29411.76	5.857	10	87.3
80	29411.76	7.268	10	76.8
100	29411.76	8.592	10	56.0
20	39215.69	2.225	10	113.6
40	39215.69	3.743	10	105.0
60	39215.69	5.073	10	92.2
80	39215.69	6.294	10	76.6
100	39215.69	7.441	10	56.0
20	49019.61	1.990	10	107.9
40	49019.61	3.347	10	103.9
60	49019.61	4.537	10	92.5
80	49019.61	5.630	10	72.2
100	49019.61	6.655	10	57.4

Table 2. Contd.

20	4901.96	6.294	20	79.5
40	4901.96	10.586	20	76.0
60	4901.96	14.348	20	51.6
80	4901.96	17.803	20	42.8
100	4901.96	21.046	20	29.1
20	9803.92	4.451	20	76.5
40	9803.92	7.485	20	101.0
60	9803.92	10.145	20	92.2
80	9803.92	12.588	20	77.5
100	9803.92	14.882	20	56.8
20	14705.88	3.634	20	103.2
40	14705.88	6.112	20	105.0
60	14705.88	8.284	20	96.1
80	14705.88	10.278	20	76.9
100	14705.88	12.151	20	56.2
20	19607.84	3.147	20	115.0
40	19607.84	5.293	20	111.5
60	19607.84	7.174	20	94.7
80	19607.84	8.901	20	76.0
100	19607.84	10.523	20	57.2
20	24509.8	2.815	20	121.5
40	24509.8	4.734	20	115.6
60	24509.8	6.416	20	98.3
80	24509.8	7.962	20	77.9
100	24509.8	9.412	20	57.2
20	3267.97	7.709	30	56.5
40	3267.97	12.965	30	62.0
60	3267.97	17.572	30	45.5
80	3267.97	21.804	30	30.0
100	3267.97	25.776	30	27.5
20	6535.95	5.451	30	92.7
40	6535.95	9.168	30	106.5
60	6535.95	12.426	30	83.0
80	6535.95	15.418	30	67.8
100	6535.95	18.227	30	41.2
20	9803.92	4.451	30	97.5
40	9803.92	7.485	30	108.4
60	9803.92	10.145	30	96.1
80	9803.92	12.588	30	76.0
100	9803.92	14.882	30	55.8
20	13071.9	3.854	30	102.1
40	13071.9	6.482	30	110.4
60	13071.9	8.786	30	96.9
80	13071.9	10.902	30	76.0
100	13071.9	12.888	30	56.2
20	16339.87	3.447	30	119.8
40	16339.87	5.798	30	113.2
60	16339.87	7.859	30	95.5
80	16339.87	9.751	30	75.6
100	16339.87	11.527	30	56.6

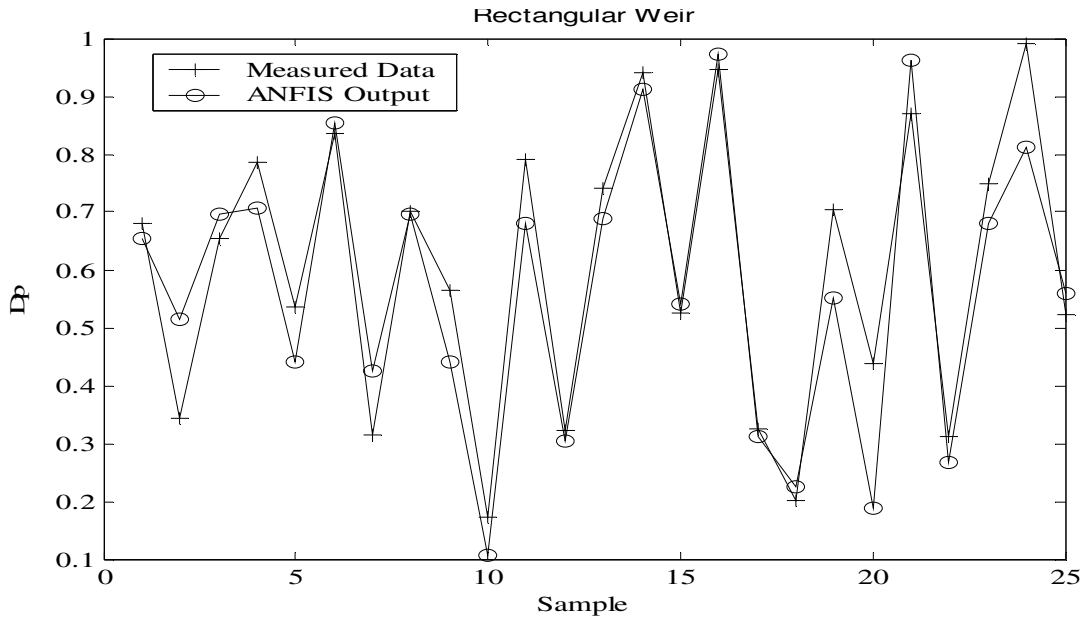

Figure 6. The predicted and measured D_p values in rectangular weir.

Table 3. Experimental data of sharp crested trapezoidal weirs.

Hd. (cm)	Re	Fj	Bw. (cm)	Dp. (cm)
20	4759.19	6.388	20.6	88.5
40	4759.19	10.743	20.6	95.5
60	4759.19	14.561	20.6	77.0
80	4759.19	18.068	20.6	58.0
100	4759.19	21.36	20.6	51.5
20	9248.98	4.582	21.2	90.5
40	9248.98	7.706	21.2	97.5
60	9248.98	10.445	21.2	91.5
80	9248.98	12.961	21.2	78.5
100	9248.98	15.322	21.2	68.5
20	13616.56	3.776	21.6	93.5
40	13616.56	6.351	21.6	111.5
60	13616.56	8.609	21.6	92.0
80	13616.56	10.682	21.6	82.5
100	13616.56	12.628	21.6	70.5
20	17825.31	3.3	22.0	97.0
40	17825.31	5.551	22.0	113.0
60	17825.31	7.524	22.0	94.5
80	17825.31	9.335	22.0	87.5
100	17825.31	11.037	22.0	71.5
20	21786.49	2.986	22.5	122.0
40	21786.49	5.021	22.5	120.0
60	21786.49	6.806	22.5	109.5
80	21786.49	8.445	22.5	91.5
100	21786.49	9.983	22.5	73.5

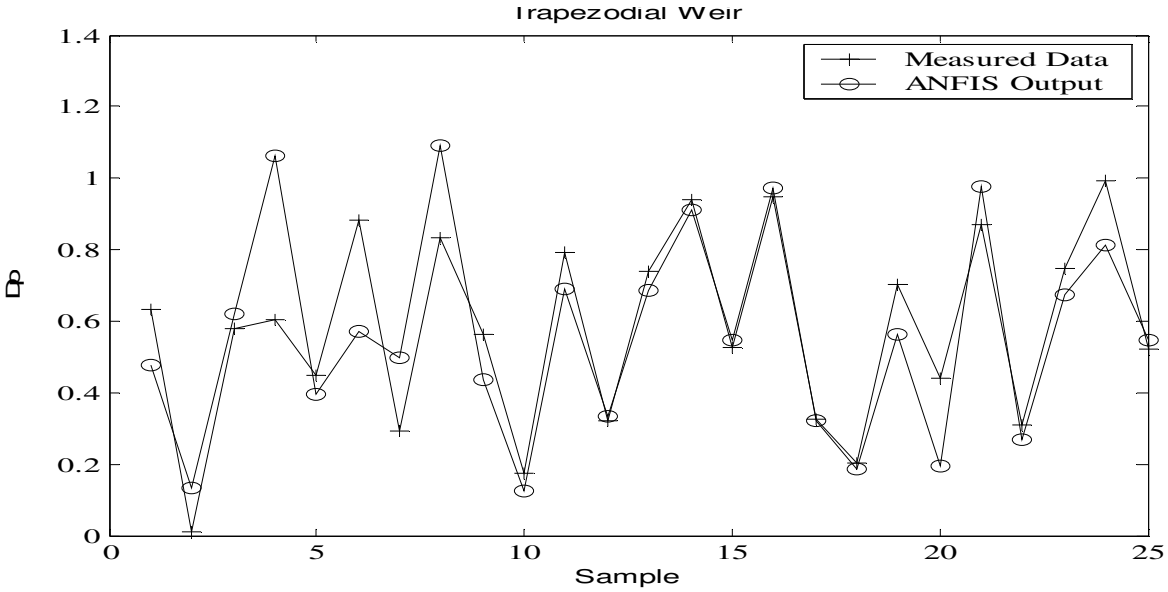

Figure 7. The predicted and measured D_p values in trapezoidal weir.

Table 4. Experimental data of sharp crested semi circular weirs.

Hd. (cm)	Re	Fj	Bw. (cm)	Dp. (cm)
20	7002.8	5.266	14.0	77.0
40	7002.8	8.857	14.0	88.0
60	7002.8	12.004	14.0	64.0
80	7002.8	14.895	14.0	44.0
100	7002.8	17.608	14.0	40.0
20	12254.9	3.981	16.0	100.0
40	12254.9	6.695	16.0	104.0
60	12254.9	9.074	16.0	90.0
80	12254.9	11.259	16.0	76.5
100	12254.9	13.311	16.0	65.5
20	16903.31	3.389	17.4	107.0
40	16903.31	5.7	17.4	110.0
60	16903.31	7.726	17.4	94.0
80	16903.31	9.587	17.4	78.5
100	16903.31	11.334	17.4	68.5
20	21312.87	3.019	18.4	110.0
40	21312.87	5.077	18.4	112.0
60	21312.87	6.881	18.4	96.0
80	21312.87	8.538	18.4	81.5
100	21312.87	10.093	18.4	72.5
20	25664.72	2.751	19.1	112.0
40	25664.72	4.626	19.1	114.5
60	25664.72	6.27	19.1	99.0
80	25664.72	7.78	19.1	87.5
100	25664.72	9.198	19.1	74.5

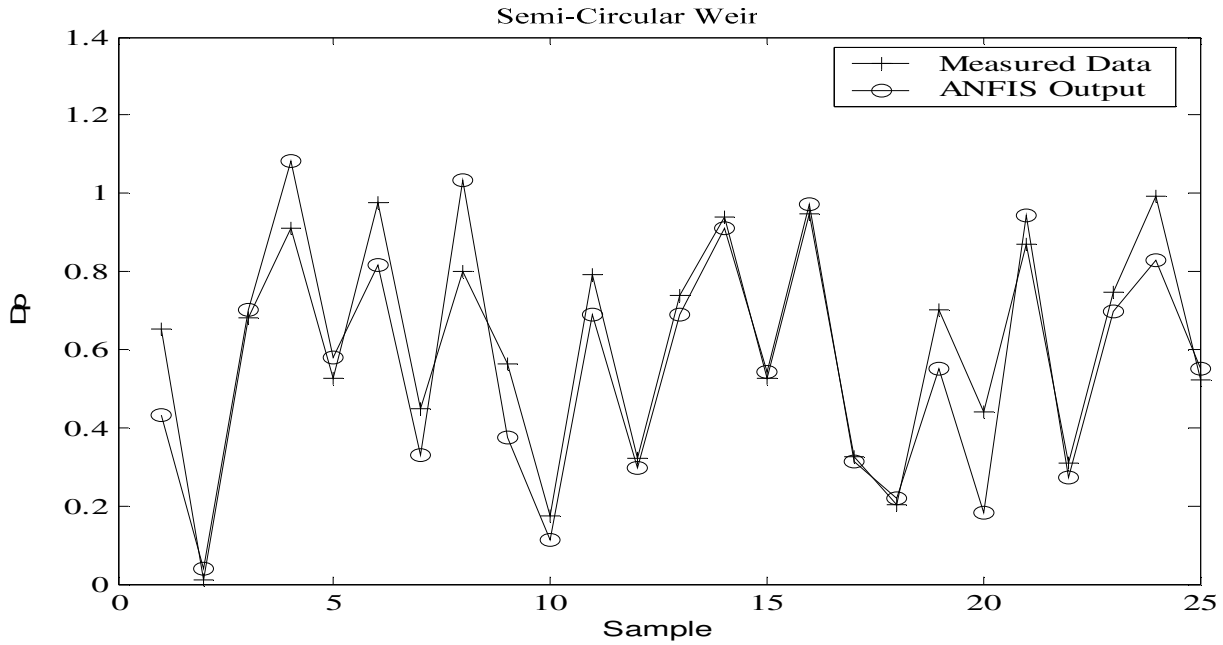

Figure 8. The predicted and measured D_p values in semi circular weir.

CONCLUSION

Aeration is very important to the quality and existence of aquatic life in water flows. The residence time of entrained air bubbles in a water body directly affects the oxygen mass transfer. The residence time is related to the bubble flow path and hence the bubble penetration depth into the downstream water pool. In this study, the penetration depth of air bubbles entrained by sharp crested weirs was modeled by using the adaptive network based fuzzy inference system (ANFIS). The obtained model was tested with experimental data. There was a good agreement between tested and experimental data in all types of sharp crested weirs. Test results showed that ANFIS can be used to estimate the penetration depth of air bubbles entrained by sharp crested weirs

ACKNOWLEDGEMENTS

The writer would like to thank Dr M. Emin Emiroglu from the Civil Engineering Department of the Firat University for their assistance, support and encouragement. Also, the writer would like to thank Dr Davut HANBAY for his technical support.

REFERENCES

Abolpour B, Javan M, Karamouz M (2007). Water allocation improvement in river basin using adaptive neural fuzzy reinforcement learning approach. Appl. Soft Computing 7(1): 265-285.

ASCE (2000). Task Committee on Application of Artificial Neural Networks in Hydrology Artificial neural networks in hydrology ASCE. J. Hydrol. Eng., 5(2): 115-137.

Avery ST, Novak P (1978). Oxygen transfer at hydraulic structures. J. Hydraulic Div, ASCE, 104(11): 1521-1540.

Baylar A (2002). Study on the effect of type selection of weir aerators on oxygen transfer. Ph.D. thesis, Firat University, Elazig, Turkey (in Turkish).

Baylar A (2003). An investigation on the use of venturi weirs as an aerator. Water Qual. Res. J. Can., 38(4): 753-767.

Baylar A, Bagatur T (2006). Experimental studies on air entrainment and oxygen content downstream of sharp-crested weirs. Water Environ. J., 20(4): 210-216.

Baylar A, Bagatur T (2000). Aeration performance of weirs. Water SA, 26(4): 521-526.

Baylar A, Emiroglu ME (2002). The effect of sharp-crested weir shape on air entrainment. Can. J. Civil Eng., 29(3): 375-383.

Baylar A, Emiroglu ME (2004). An Experimental Study of Air Entrainment and Oxygen Transfer at a Water Jet from a Nozzle with Air Holes. Water Environ. Res., pp. 76- 231.

Baylar A, Hanbay D, Ozpolat E (2007). Modeling Aeration Efficiency of Stepped Cascades by Using ANFIS, CLEAN - Soil, Air, Water, 35(2): 186-192.

Emiroglu ME (2010). "Estimating Trajectory, Jet Expansion and Penetration Depth of Free Overall in Different Weir Types". J. Hydrol Hydromechanics, in Press.

Emiroglu ME, Baylar A (2003). Experimental study of the influence of different weir types on the rate of air entrainment Canada. Water Qual. Res. J., 38(4): 769-783.

Gulliver JS, Rindels AJ (1993). Measurement of Air-Water Oxygen Transfer at Hydraulics Structures". J. Hydraulic. Eng. ASCE, 119(3): 328-349.

Gulliver JS, Thene JR, Rindels AJ (1990). Indexing Gas Transfer in Self-Aerated Flows". J. Environ. Eng. ASCE, 116(3): 503-523.

Hanbay D, Türkoğlu İ, Demir Y (2006a). “Complex Systems Modeling by Using ANFIS”, TAINN, 83-90, Muğla, Turkey.

Hanbay D, Türkoğlu İ, Demir Y (2006b). “A Wavelet Neural Network for Intelligent Modeling”, TAINN, 175-182, Muğla, Turkey.

Ito A, Yamagiwa KT, Yoshida M, Ohkowa A (2000). “Maximum penetration depth of air bubbles entrained by vertical liquid jet”. J.

Chem. Eng. Jpn., 33(6): 898-900.
Jang JSR (1993). ANFIS: Adaptive Network-Based Fuzzy Inference Systems. IEEE, Trans. Syst. Man. Cybern. 23(3): 665-685.
Kisi O (2004a). River flow modeling using artificial neural networks. J. Hydrologic. Eng. ASCE, 9(1): 60-63.
Kisi O (2004b). Multi-layer perceptions with Levenberg–Marquardt optimization algorithm for suspended sediment concentration prediction and estimation. Hydrol. Sci. J., 49(6): 1025-1040.
Kulkarni AD (2001). Computer Vision and Fuzzy Neural Systems. Prentice Hall NJ.
Wormleaton PR, Tsang CC (2000). Aeration performance of rectangular platform labyrinth weirs. ASCE. J. Environ. Eng., 126(5): 456-465.